JOURNAL OF GEOPHYSICAL RESEARCH
Solid Earth
JGR
JOURNAL
Volume 119 • Issue 8 • August 2014 • Pages 6113–6704

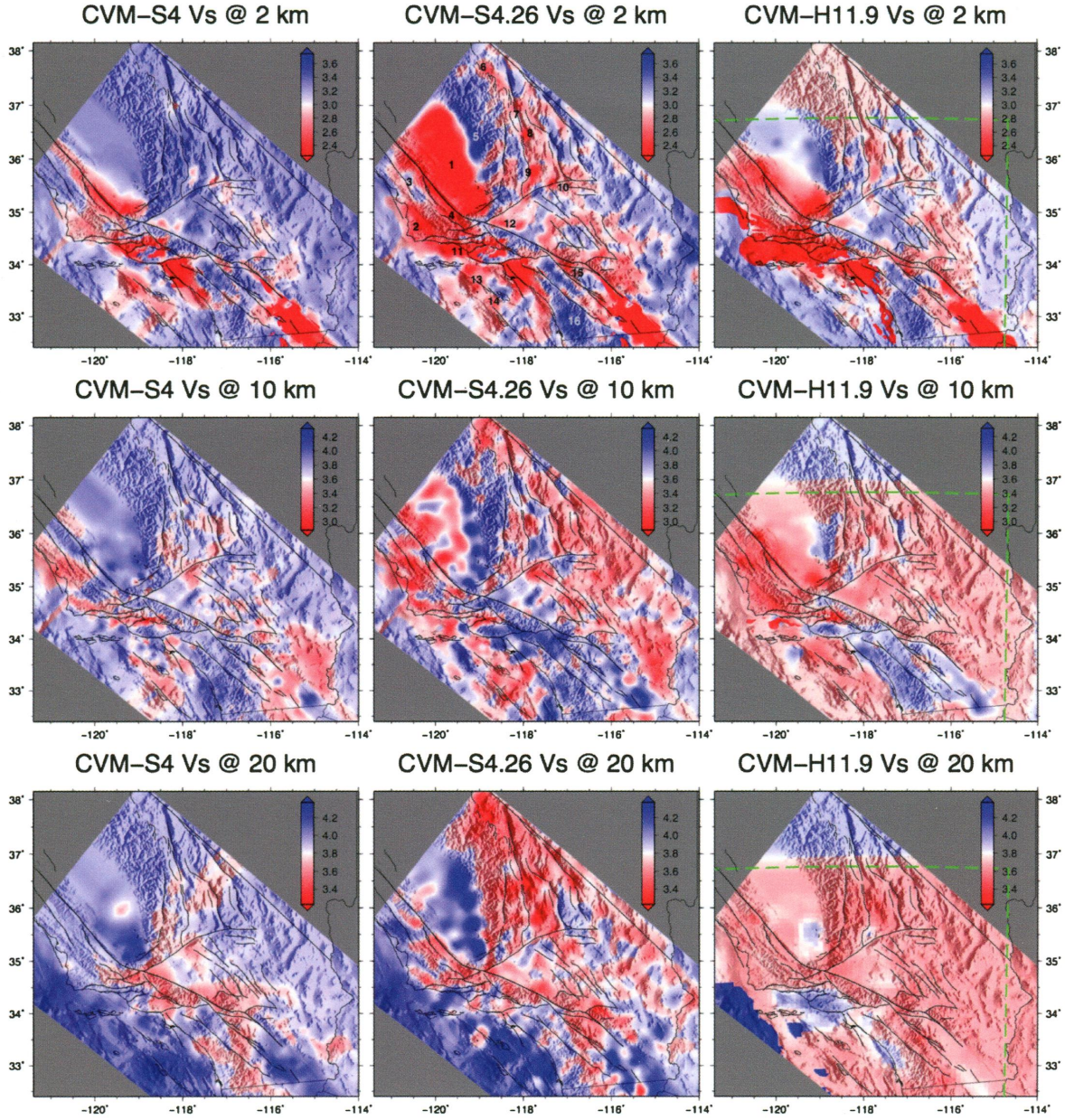

AGU PUBLICATIONS
WILEY

Journal of Geophysical Research Solid Earth

Volume 119 Issue 8 August 2014
JGREA2(8) 6113–6704 (2014)
ISSN 2169-9313 (print); ISSN 2169-9356 (Online)

The online article is the official version and may contain additional content not available in this print issue. To access the full article, including multimedia, enhanced figures, supporting information, and other nonprinted content, go to http://wileyonlinelibrary.com/journal/jgrb.

Geomagnetism and Paleomagnetism/Marine Geology and Geophysics

6113 *E. C. Ferré, J. W. Geissman, F. Demory, J. Gattacceca, M. S. Zechmeister, and M. J. Hill*
Coseismic magnetization of fault pseudotachylytes: 1. Thermal demagnetization experiments (doi 10.1002/2014JB011168)

6136 *Liao Chang, Andrew P. Roberts, Michael Winklhofer, David Heslop, Mark J. Dekkers, Wout Krijgsman, John D. Fitz Gerald, and Paul Smith*
Magnetic detection and characterization of biogenic magnetic minerals: A comparison of ferromagnetic resonance and first-order reversal curve diagrams (doi 10.1002/2014JB011213)

6159 *Peter Franek, Jürgen Mienert, Stefan Buenz, and Louis Géli*
Character of seismic motion at a location of a gas hydrate-bearing mud volcano on the SW Barents Sea margin (doi 10.1002/2014JB010990)

Chemistry and Physics of Minerals and Rocks/Volcanology

6178 *Olivier Galland, Steffi Burchardt, Erwan Hallot, Régis Mourgues, and Cédric Bulois*
Dynamics of dikes versus cone sheets in volcanic systems (doi 10.1002/2014JB011059)

6193 *Johann F. A. Diener and Åke Fagereng*
The influence of melting and melt drainage on crustal rheology during orogenesis (doi 10.1002/2014JB011088)

6211 *Hiroki Goto, Masaatsu Aichi, Tomochika Tokunaga, Hajime Yamamoto, Toyokazu Ogawa, and Tomoyuki Aoki*
Quantitative study on experimentally observed poroelastic behavior of Berea sandstone in two-phase fluid system (doi 10.1002/2013JB010937)

6229 *Atsuko Namiki, Carolina Muñoz-Saez, and Michael Manga*
El Cobreloa: A geyser with two distinct eruption styles (doi 10.1002/2014JB011009)

6249 *Zhihong Zhao and Alasdair Skelton*
An assessment of the role of nonlinear reaction kinetics in parameterization of metamorphic fluid flow (doi 10.1002/2014JB011016)

6263 *Shimin Liu and Satya Harpalani*
Evaluation of in situ stress changes with gas depletion of coalbed methane reservoirs (doi 10.1002/2014JB011228)

6277 *Chao Wang, Akira Yoneda, Masahiro Osako, Eiji Ito, Takashi Yoshino, and Zhenmin Jin*
Measurement of thermal conductivity of omphacite, jadeite, and diopside up to 14GPa and 1000 K: Implication for the role of eclogite in subduction slab (doi 10.1002/2014JB011208)

6288 *P. S. Lang, A. Paluszny, and R.W. Zimmerman*
Permeability tensor of three-dimensional fractured porous rock and a comparison to tracemap predictions (doi 10.1002/2014JB011027)

6308 *Andrea Parmigiani, Christian Huber, and Olivier Bachmann*
Mush microphysics and the reactivation of crystal-rich magma reservoirs (doi 10.1002/2014JB011124)

Seismology

6323 *Gregory C. McLaskey and David A. Lockner*
Preslip and cascade processes initiating laboratory stick slip (doi 10.1002/2014JB011220)

6337 *Andrew J. Smith, Peter B. Flemings, Xiaoli Liu, and Kristopher Darnell*
The evolution of methane vents that pierce the hydrate stability zone in the world's oceans (doi 10.1002/2013JB010686)

6357 *Youyi Ruan, Donald W. Forsyth, and Samuel W. Bell*
Marine sediment shear velocity structure from the ratio of displacement to pressure of Rayleigh waves at seafloor (doi 10.1002/2014JB011162)

0148-0227JB-119-8

6372 *Madan M. Dixit, Sanjay Kumar, R. D. Catchings, K. Suman, Dipankar Sarkar, and M. K. Sen*
Seismicity, faulting, and structure of the Koyna-Warna seismic region, Western India from local earthquake tomography and hypocenter locations (doi 10.1002/2014JB010950)

6399 *Sébastien Chevrot, Antonio Villaseñor, Matthieu Sylvander, Sébastien Benahmed, Eric Beucler, Glenn Cougoulat, Philippe Delmas, Michel de Saint Blanquat, Jordi Diaz, Josep Gallart, Franck Grimaud, Yves Lagabrielle, Gianreto Manatschal, Antoine Mocquet, Hélène Pauchet, Anne Paul, Catherine Péquegnat, Olivier Quillard, Sandrine Roussel, Mario Ruiz, and David Wolyniec*
High-resolution imaging of the Pyrenees and Massif Central from the data of the PYROPE and IBERARRAY portable array deployments (doi 10.1002/2014JB010953)

6421 *En-Jui Lee, Po Chen, Thomas H. Jordan, Phillip B. Maechling, Marine A. M. Denolle, and Gregory C. Beroza*
Full-3-D tomography for crustal structure in Southern California based on the scattering-integral and the adjoint-wavefield methods (doi 10.1002/2014JB011346)

6452 *Stephen S. Gao and Kelly H. Liu*
Mantle transition zone discontinuities beneath the contiguous United States (doi 10.1002/2014JB011253)

6469 *Alexey Sukhovich, Jean-Olivier Irisson, Julie Perrot, and Guust Nolet*
Automatic recognition of *T* and teleseismic *P* waves by statistical analysis of their spectra: An application to continuous records of moored hydrophones (doi 10.1002/2013JB010936)

6486 *Saeko Kita, Junichi Nakajima, Akira Hasegawa, Tomomi Okada, Kei Katsumata, Youichi Asano, and Takeshi Kimura*
Detailed seismic attenuation structure beneath Hokkaido, northeastern Japan: Arc-arc collision process, arc magmatism, and seismotectonics (doi 10.1002/2014JB011099)

6512 *Yajing Liu*
Source scaling relations and along-strike segmentation of slow slip events in a 3-D subduction fault model (doi 10.1002/2014JB011144)

Geodesy and Gravity/Tectonophysics

6534 *Caleb W. Holyoke, Andreas K. Kronenberg, Julie Newman, and Christopher Ulrich*
Rheology of magnesite (doi 10.1002/2013JB010541)

6558 *P. Vernant, R. Bilham, W. Szeliga, D. Drupka, S. Kalita, A. K. Bhattacharyya, V. K. Gaur, P. Pelgay, R. Cattin, and T. Berthet*
Clockwise rotation of the Brahmaputra Valley relative to India: Tectonic convergence in the eastern Himalaya, Naga Hills, and Shillong Plateau (doi 10.1002/2014JB011196)

6572 *E. Chaussard, R. Bürgmann, M. Shirzaei, E. J. Fielding, and B. Baker*
Predictability of hydraulic head changes and characterization of aquifer-system and fault properties from InSAR-derived ground deformation (doi 10.1002/2014JB011266)

6591 *Adam Bailey, Rosalind King, Simon Holford, Joshua Sage, Guillaume Backe, and Martin Hand*
Remote sensing of subsurface fractures in the Otway Basin, South Australia (doi 10.1002/2013JB010843)

6613 *Halfdan Pascal Kierulf, Holger Steffen, Matthew James Ross Simpson, Martin Lidberg, Patrick Wu, and Hansheng Wang*
A GPS velocity field for Fennoscandia and a consistent comparison to glacial isostatic adjustment models (doi 10.1002/2013JB010889)

6630 *Jill Pearse, Vern Singhroy, Sergey Samsonov, and Junhua Li*
Anomalous surface heave induced by enhanced oil recovery in northern Alberta: InSAR observations and numerical modeling (doi 10.1002/2013JB010885)

6650 *Alex Copley, Supriyo Mitra, R. Alastair Sloan, Sharad Gaonkar, and Kirsty Reynolds*
Active faulting in apparently stable peninsular India: Rift inversion and a Holocene-age great earthquake on the Tapti Fault (doi 10.1002/2014JB011294)

6667 *Jingyi Chen, Howard A. Zebker, Paul Segall, and Asta Miklius*
The 2010 slow slip event and secular motion at Kīlauea, Hawai`i, inferred from TerraSAR-X InSAR data (doi 10.1002/2014JB011156)

6684 *W. Sharples, M. A. Jadamec, L. N. Moresi, and F. A. Capitanio*
Overriding plate controls on subduction evolution (doi 10.1002/2014JB011163)

Cover. In *Lee et al.* [doi:10.1002/2014JB011346], image shows shear-wave velocities of southern California crust obtained through ray-theoretical travel-time tomography (CVM-S4, left column), adjoint tomography (CVM-H11.9, right column) and full-3D tomography (F3DT) (CVM-S4.26, center column) at 2-km (top row), 10-km (center row) and 20-km (bottom row) depths. Red colors indicate relatively lower shear-wave velocities and blue colors indicate relatively higher shear-wave velocities. Black solid lines show major mapped faults in this area. Green dash-line boxes on the right column indicate the area of the adjoint tomography of *Tape et al.* [2009; 2010]. Numbers shown in the top row, center column, indicate locations of geological features imaged through F3DT. See pp. 6421-6451.